In Situ Hybridization and Characterization of Fibrous Hydroxyapatite/Chitosan Nanocomposite

C. Y. Zhang,[1,2] J. Chen,[2] Z. Zhuang,[1] T. Zhang,[1] X. P. Wang,[1] Q. F. Fang[1]

[1]*Key Laboratory of Materials Physics, Institute of Solid State Physics, Chinese Academy of Sciences, Hefei 230031, People's Republic of China*
[2]*School of Pharmacy, Anhui Traditional Chinese Medical College, Hefei 230038, People's Republic of China*

Received 30 September 2010; accepted 14 June 2011
DOI 10.1002/app.35103
Published online 4 October 2011 in Wiley Online Library (wileyonlinelibrary.com).

ABSTRACT: Nano-fibrous hydroxyapatite/chitosan (HA/CS) composites with HA contents of 0–70 wt % were prepared by *in situ* hybridization with a preprepared chitosan film as semipermeable membrane to slow down the hybridization process. The phase composition, microstructure, and morphology of the composites were characterized by means of Fourier transform infrared spectroscopy, X-ray diffraction, and high-resolution transmission electron microscopy. It was found that the *in situ* prepared inorganic phase was hydroxyapatite nano-fibers that were uniformly dispersed in the chitosan matrix. The average diameter of the fibers were about 3 nm, while the length of the fibers increases from 20 to 60 nm when the hydroxyapatite content increased from 10 to 70 wt %. The compressive strength and Young's modulus of these nano-fibrous HA/CS composites increased with the increasing HA content and reached the highest values of 170 and 1.7 GPa, respectively, at the HA content of 50–70 wt %, which were much higher than the values of samples prepared by coprecipitation. © 2011 Wiley Periodicals, Inc. J Appl Polym Sci 124: 397–402, 2012

Key words: fibrous hydroxyapatite; chitosan; HA/CS composites; *in situ* hybridization

INTRODUCTION

Natural bone is an organic–inorganic composite, in which hydroxyapatite (HA, $Ca_{10}(PO_4)_6(OH)_2$) nanocrystallites and collagen fibrils are well organized at the nano-scaled level.[1,2] Therefore, the composite with nano-HA crystallites dispersed in synthetic or natural polymer matrices has been considered as a potential candidate as bone substitutes.

Nowadays, natural polymers[3,4] and their derivatives[5] are preferred to synthetic polymers owing to their biocompatibility, biodegradability, and biological activity. Chitosan (CS) is an *N*-deacetylation product of chitin consisting of glucosamine and *N*-acetylglucosamine units linked through β-D-1,4-glycosidic bonds.[6] Owing to the unique properties such as biodegradability by enzymes in human body, nontoxicity of the degradation product, antibacterial effect, and biocompatibility, CS-based biomedical materials have attracted much attention.[7–10] However, the lack of bone-bonding bioactivity and poor mechanical properties at the high humidity condition limit the use of CS-based biomedical materials in the field of bone tissue engineering. On the other side, although the long-term biocompatibility and the favorable interaction with soft tissue and bone have been evidenced for the synthetic HA in the process of application as bone substitutes,[11–15] the brittleness makes it impossible for HA to be used for load-bearing bone repair and substitute.

Therefore, the nano-HA/CS composite materials are expected to possess the favorable properties of both CS and HA. It was reported[13–16] that the HA/CS composites showed better biocompatibility, tissue regenerative efficacy, osteoconductivity, and favorable bonding ability with surrounding host tissues than the pure CS scaffolds. At the same time, addition of HA particles to CS reduces the water absorption and increases the mechanical property of the composites at high humidity condition.[17]

HA/CS composites have been synthesized with various methods, including mechanical mixing of HA powders in CS solution,[18,19] coating of HA particles onto CS sheet,[20] coprecipitation,[21–23] and alternate soaking process.[24] In these approaches except for coprecipitation, the inorganic particles can be not uniformly distributed at the nano-scale in the organic matrix, which would lead to poor mechanical properties. Although the coprecipitation method did result in uniformly dispersed nano-sized HA crystallites, but the precipitation was too fast so that disordered microstructure was generally obtained. In contrast to the aforementioned methods, the *in situ*

Correspondence to: Q. F. Fang (qffang@issp.ac.cn).
Contract grant sponsor: Natural Science Foundation of Anhui Province; contract grant number: 10040606Q36.

hybridization[17,25,26] method is an effective way to ensure uniform dispersion of inorganic phase in the organic matrix and ordered microstructure, resulting in good mechanical properties of the composite materials.

In the system of $Ca(OH)_2$-H_3PO_4-H_2O, HA is the most basic calcium orthophosphate,[27] and insoluble in neutral and basic medium, while the pH value for CS precipitation is generally close to 6.0.[28] Therefore it is possible to synthesize HA/CS composites by manipulating the pH value in the precursor solution. In this article, the *in situ* hybridization method was exploited to prepare nano-fibrous hydroxyapatite/chitosan (HA/CS) composites with HA contents of 0–70 wt %, where the nano-fibrous HA phase was *in situ* synthesized using $Ca(OH)_2$ and H_3PO_4 as precursors in the CS matrix and using the CS film as a semipermeable membrane to control the precipitation speed. The microstructure and mechanical properties were characterized and the corresponding mechanism was discussed.

MATERIALS AND METHODS

Materials

Biomedical grade CS (viscosity-average molecular weight 4.5×10^5) with 95% degree of the deacetylation was supplied by Bomei Bioengineering (China). $Ca(OH)_2$, 85% orthophosphoric acid (H_3PO_4) solution, and acetic acid (CH_3COOH, reagent grade) were purchased from Sinopharm Chemcial Reagent (China).

Preparation of CS film

Before synthesis of nano-HA/CS composite, a CS semipermeable membrane was prepared as follows. At first, an appropriate amount of 2 wt % CS solutions was prepared by dissolving CS into 1 vol % acetic acid and continuously stirring at room temperature for 6 h. The obtained CS solution was filtered to remove undissolved material and then degassed by keeping the solution in a vacuum oven for 3 h to remove the trapped air bubbles. The clear and transparent CS solution was cast on the inner surface of a dialysis bag ($\leq$12,000 Da, China) and the redundant CS solution was poured out. After soaking in a solution of 3 wt % NaOH aqueous solution for 30 min and washing to neutralization in deionized water, the resultant CS film was dried in vacuum. These processes were repeated two to three times to synthesize a thick and seamless CS semipermeable membrane.

Preparation of nano-fibrous HA/CS composites

At first, an appropriate amount of 1 wt % CS solution was prepared by dissolving CS into 1 vol % acetic acid and continuously stirring at room temperature for 6 h. Then the corresponding amount of 6 wt % H_3PO_4 aqueous solution was slowly added to the transparent CS solution with continuous stirring. Subsequently the obtained H_3PO_4-CS solution was added dropwise to a suspension of 2 wt % $Ca(OH)_2$ with vigorous stirring at 37°C. The amount of $Ca(OH)_2$ suspension was weighted so that the Ca/P ratio is 1.67 as same as in the HA phase. The resulting slurry was stirred continuously for 6 h after the titration and then incubated at room temperature for 24 h. The pH value of the resulting slurry after titration was about 5.1–6.0 corresponding to different HA contents. The aged CS-$Ca(OH)_2$-H_3PO_4 slurry was poured into a CS semipermeable membrane coated dialysis bag and then immersed into a 2 wt % NaOH aqueous solution to *in situ* hybridize the HA/CS composite. The pH value of the slurry after *in situ* hybridization was about 12. After these treatments, the products were filtered and washed to neutralization with deionized water and at last dried in a vacuum oven at 60°C for 24 h.

TABLE I
The Dosage of Reagents for the Preparation of CS/HA Nanocomposites

HA/CS ratio (wt %)	CS (g)	$Ca(OH)_2$ (g)	H_3PO_4 (g)
10/90	4.5	0.37	0.294
20/80	4	0.74	0.588
30/70	2.4	0.74	0.588
50/50	2	1.48	1.176
70/30	0.87	1.48	1.176

The amounts of all reagents were scaled according to the final HA/CS weight ratios of 10/90, 20/80, 30/70, 50/50, and 70/30, and listed in Table I. For comparison, another kind of HA/CS composite was prepared by coprecipitation method as described elsewhere.[22]

Synthesis of pure nano-HA

The pure nano-HA particles were synthesized by wet chemical method using $Ca(OH)_2$ and H_3PO_4 as precursors. This reaction can be written as follows.[29]

$$10Ca(OH)_2 + 6H_3PO_4 \longrightarrow Ca_{10}(PO_4)_6(OH)_2 + 18H_2O \quad (pH > 10) \qquad (1)$$

With the atomic ratio Ca/P $\approx$ 1.67, an appropriate amount of 9 wt % H_3PO_4 aqueous solution was slowly titrated into the 3 wt % $Ca(OH)_2$ suspension at 37°C under continuous stirring, while the pH value of the solution was adjusted to be a little greater than 10 by controlling the titration speed of H_3PO_4 aqueous solution. After titration, the precipitates were

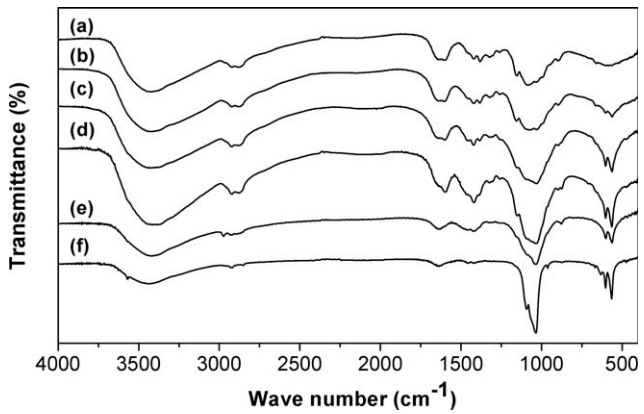

Figure 1 FT-IR spectra of pure CS (a), 10 wt % (b), 30 wt % (c), 50 wt % (d), and 70 wt % (e) nano-fibrous HA/CS composites, and pure HA (f), respectively.

aged at room temperature for 24 h. The nano-HA particles were obtained by washing these precipitates with deionized water and drying at 60°C.

Characterization

The Fourier transform infrared (FT-IR) spectroscopy measurements were taken in a Nicolet Nexus spectrometer operating in transmission mode in the range from 4000 to 400 cm^{-1} to confirm the chemical composition and the possible interaction between HA and CS in the composites. The powder samples were mixed with KBr powders and pressed into discs for the FT-IR measurement. X-ray diffraction (XRD) was exploited to identify crystalline phases in a Philips X'pert PRO X-ray diffractometer with Cu Kα radiation. The XRD patterns were collected at room temperature in the 2θ scanning range from 10° to 60° with a step of 0.033°. Transmission electron microscopy (TEM, JEOL-2010) were exploited to detect the morphologies of composites and the grown HA crystals.

Mechanical properties of composites were evaluated by compressive measurement with a CMT4204 mechanical tester (SANS, China) at a constant crosshead speed of 1 mm min^{-1}. The samples for compression measurement were prepared by pressing the powders of nano-fibrous HA/CS composites in a cylindrical stainless steel mold at 100°C under a pressure of 200 MPa. The Young's modulus was determined from the slope of initial linear elastic portion in stress–strain curves. Both compressive strength and modulus data were obtained by averaging over five specimens prepared at same conditions.

RESULTS AND DISCUSSION

FT-IR analysis

Figure 1 shows the FTIR spectra of CS (Curve a), nano-fibrous HA/CS composites with different HA content (Curves b–e), and pure HA (Curve f). The FTIR spectrum of pure CS (Curve a) exhibits characteristic band around 3425 cm^{-1} corresponding to the stretching vibration of hydroxyl group and the characteristic bands at about 1660 and 1600 cm^{-1} corresponding to the amides I and II. Additionally, the bands at 2930–2850 cm^{-1} correspond to the —CH backbone stretching vibrations and the bands at 1153, 1084, and 1028 cm^{-1} correspond to the C—O stretching vibrations pertinent to the glucosamine unit.[30,31] The inorganic phase (Curve f) displays absorption bands quite similar to the characteristic bands of the stoichiometric HA. The bands at 1092, 1036, 962, 604, and 565 cm^{-1} correspond to different vibration modes of PO_4^{3-} group in HA, and band at 3569 cm^{-1} can be assigned to the stretching vibrations of OH^- group.[32,33]

In the FTIR spectra of nano-HA/CS composites (Curves b–e), the entire characteristic bands of HA and CS were observed, except for the characteristic band of the hydroxyl group of HA at the 3569 cm^{-1}. Furthermore, the characteristic bands of the Amides I and II of CS, which correspond to the C=O stretching vibration and the *N*—H in plane bending vibration, respectively, changed their relative strength when the HA content changed, as shown in Figure 2. The ratio between the peak strengths of the amide bands II and I is about 1.36, 1.47, 1.66, and 2.43 when the HA content is 0 (pure CS), 10, 30, and 50 wt %, respectively, indicating that the relative strength of the amide band I becomes more and more weak. These phenomena imply that the number of un-affected C=O bonds in CS decreases with increasing HA content, because the strength of the FTIR spectrum is proportional to the mass ratio of the corresponding materials. This fact suggests that there might be mutual interactions between the organic and inorganic components in the HA/CS composites, which were possibly the hydrogen bonding between the hydroxyl groups of HA and the C=O functional groups of CS molecules.[34]

XRD analysis

X-ray diffraction patterns of pure CS (Curve a), *in situ* formed nano-fibrous HA/CS composites (Curves b–e) and pure HA (Curve f) prepared in our lab were shown in Figure 3. Pure CS was characterized by a broad peak approximately at 20° that can be assigned to chains aligned through intermolecular interactions. The main diffraction peaks of pure HA synthesized in this study were located at 25.9°, 31.9°, 32.2°, 32.9°, 34.1°, 35.1°, and 40.1°, in coincidence with the data for standard HA phase (JCPDS No. 09-0432).[35] In all *in situ* hybridized nano-fibrous HA/CS composites the peak at 20° corresponding to the CS is present but decreases in

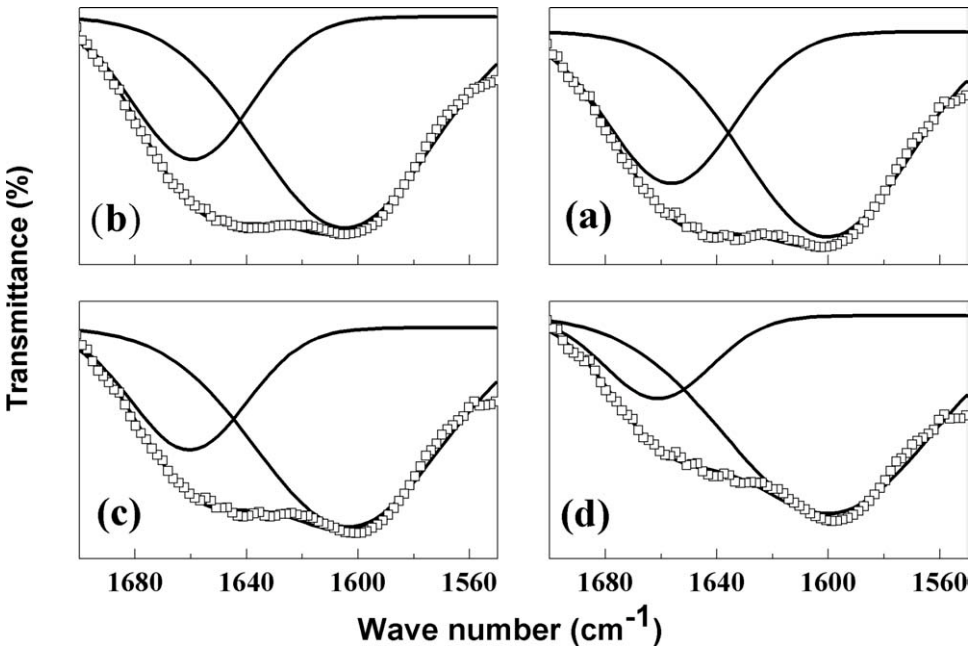

Figure 2 The enlarged FT-IR spectra of pure CS (a), 10 wt % (b), 30 wt % (c), and 50 wt % (d), nano-fibrous HA/CS composites respectively.

height with the increasing content of HA. When the HA content is 10%, besides the CS peak at 20°, only two peaks appeared at 25.8° and 32°, corresponding to the (002) diffraction and the overlapped diffractions of, (300), (211), and (112) of HA, respectively, according to standard HA phase (JCPDS No. 09-0432),[35] and other peaks of HA is absent owing to the low content of HA in the nano-fibrous HA/CS composite. When the HA content is greater than 20%, all HA peaks similar to the pure HA phase are detected, implying that the HA phase was *in situ* formed in the hybrid composites. It can be seen that with the increasing HA content, the HA peaks become sharper, indicating an increase in grain size of nano-HA. According to the Scherrer equation, the mean grain size of nano-HA in the *in situ* hybridized HA/CS nanocomposites is calculated as 20, 28, 35, and 48 nm corresponding to the HA content of 10, 30, 50, and 70 wt %, respectively.

Microscopy analysis

TEM micrographs of nano-HA and HA/CS composites were shown in Figure 4. It can be seen that the pure nano-HA particles [Fig. 4(a)] exhibit small rod-like nano-crystallites with a mean size of about 45 nm in length and 20 nm in width. These HA crystallites display a relatively uniform morphology. Typical TEM image of HA in the HA/CS composites obtained by coprecipitation method [Fig. 4(b)] shows a spindly shuttle-like morphology with an average size of about 200 nm in length and 35 nm in width, similar to the results reported in Ref. [22]. The HA crystallites in the *in situ* hybridized HA/CS composite [Fig. 4(c–e)] are nano-sized fibers with a high mean aspect ratio (the diameter of fibers is about 3 nm) and a uniform dispersion in the CS matrix. When the HA content increases from 30 to 70 wt %, the length of HA fibers increases continuously from about 30 to 60 nm while keeping the diameter almost constant.

The high resolution TEM image of the nano-HA fibers in the *in situ* hybridized HA/CS composite [Fig. 4(f)] indicates that the distance between the atomic layer perpendicular to the length direction of the fibers is about 0.34 nm, which corresponds to the spacing of the (002) plane of HA crystals. This means that the growth of nano-HA crystallites in the

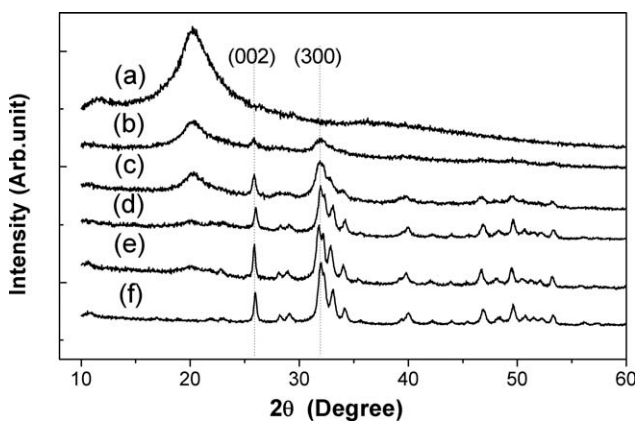

Figure 3 XRD patterns of pure CS (a), 10 wt % (b), 30 wt % (c), 50 wt % (d), and 70 wt % (e) nano-fibrous HA/CS composites, and pure HA (f), respectively.

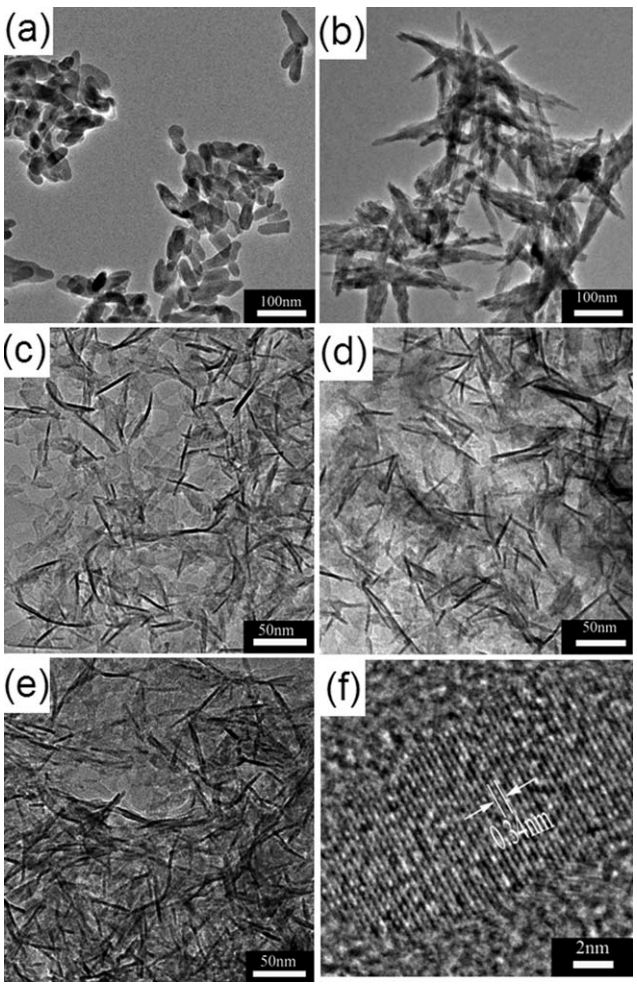

Figure 4 TEM images of pure HA (a), 50 wt % HA/CS nanocomposites fabricated by coprecipitation (b), and 30 wt % (c), 50 wt % (d), 70 (e) wt % nano-fibrous HA/CS composites fabricated by *in situ* hybridization, respectively, and the HRTEM image of a HA fiber in the *in situ* hybridized 70 wt % nano-fibrous HA/CS composite (f).

CS matrix prefers in the c-axis and that the length direction of the nano-HA fibers is along the c-axis.

Because the preprepared CS membrane was used as semipermeable membrane, small ions such as Na^+, OH^-, H^+ and so on, can diffuse through the CS membrane owing to the concentration gradient, but larger ions such as Ca^{2+} and $H_2PO_4^-$ are difficult to migrate through the CS membrane and the CS molecules can not migrate through at all. In general the OH^- and H^+ ions migrate much faster than the other ions. When OH^- ions migrate into the resulting solution through the CS membrane and encountered the CS-NH_3^+, Ca^{2+}, and $H_2PO_4^-$, the CS was precipitated at first and then the calcium phosphate forms and converts to HA after aging. The HA was *in situ* formed on the CS chains by coordinate bonding. Because the Ca^{2+} and $H_2PO_4^-$ ions are well-distributed in the resulting solution, the obtained HA/CS composites are uniform.

As well known, the pH value for the formation of HA must be more than 10. However, owing to the obstruction of the semipermeable CS membrane the concentration of OH^- within the resulting slurry is low and the adsorption of OH^- ions onto the surface of the HA nuclei was limited. This will slow down the nucleation rate and the subsequent growth of HA crystallites in terms of the kinetics of the crystal growth process.[36] On the other hand, in the case of dilute ion concentration and slow nucleation rate, the crystallites would grow preferentially in anisotropic growth direction along the high energy facets from the view of the quasi-equilibrium thermodynamic state.[37] The formation of HA nano-fibers can be ascribed to the anisotropic growth of the HA crystallites in such a low concentration. However, for the coprecipitated HA/CS composite without CS membrane as semipermeable membrane, the high concentration of OH^- promotes the HA crystallite growth in isotropic or weak-anisotropic direction and thus only spindly shuttle-like HA crystallites were formed.

Mechanical properties

The mechanical properties of nano-HA/CS composites were evaluated by compressive measurements. Compressive strength and Young's modulus as a function of HA content in nano-fibrous HA/CS composites prepared by *in situ* hybridization were illustrated in Figure 5, where the results of the samples prepared by coprecipitation are also shown for comparison. The compressive strength and Young's modulus of the nano-fibrous HA/CS composites prepared by *in situ* hybridization increase from 87 to 174 MPa and from 0.6 to 1.7 GPa, respectively, when the HA content increases from 10 and 70 wt %. This variation is linear at low HA content and seems to become saturated at high HA content. But for

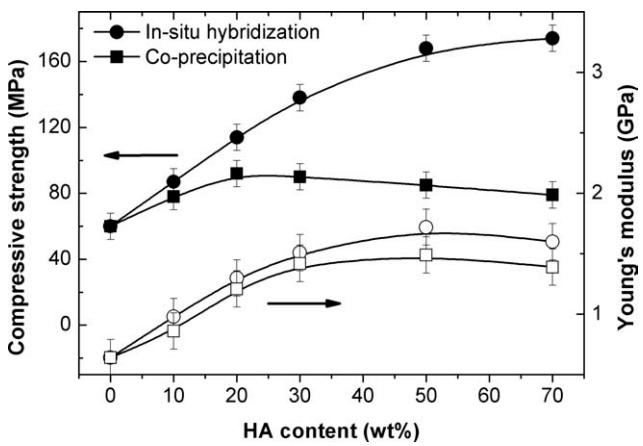

Figure 5 The dependence of compressive strength and Young's modulus upon the HA content in nano-fibrous HA/CS composite and co-precipitation HA/CS composite.

samples prepared by coprecipitation, the compressive strength was 90, 85, and 80 MPa when the HA content was 30, 50, and 70 wt %, respectively. It is clear that the compressive strength of the HA/CS composites prepared by *in situ* hybridization are obviously higher than the samples prepared by coprecipitation. This enhancement would be attributed partially to the fibrous morphology of HA crystallites and partially to the chemical interactions between HA and CS, because the proper stress transfer occurring between the filler and the matrix governs the mechanical characteristics of organic/inorganic hybridized composites.[38,39] However, the Young's modulus of the coprecipitated composite is only a little smaller than that of the *in situ* hybridized composite.

CONCLUSIONS

In this study, nano-fibrous HA/CS composites have been fabricated by *in situ* hybridization with the help of preprepared CS semipermeable film. FT-IR, XRD, and TEM analysis identify that the inorganic phase in these composites were HA nano-fibers with a diameter of about 3 nm and a uniform dispersion in the composites. Incorporation of HA nano-fibers into CS matrix significantly enhances the mechanical properties of the composites. When HA content increases from 10 to 70 wt %, the compressive strength and Young's modulus increase from 87 to 170 MPa and from 1.0 to 1.7 GPa, respectively, which were higher than the samples prepared by coprecipitation. These improvements can be mainly ascribed to fibers reinforcement and the chemical bonding between fibrous HA and the CS matrix. The present study has demonstrated the feasibility of this bio-mimetic approach to prepare high quality nano-fibrous HA/CS composites.

The authors appreciate Dr. Chun Li at Nanchang Hangkong University for her help in the compression experiments.

References

1. Du, C.; Cui, F. Z.; Zhang, W.; Feng, Q. L.; Zhu, X. D.; De Groot, K. J Biomed Mater Res 2000, 50, 518.
2. Kikuchi, M.; Itoh, S.; Ichinose, S.; Shinomiya, K.; Tanaka, J. Biomaterials 2001, 22, 1705.
3. Grodzinski, J. J React Funct Polym 1999, 39, 99.
4. Hutmacher, D. W. Biomaterials 2000, 21, 2529.
5. Chang, M. C.; Tanaka, J. Biomaterials 2002, 23, 3879.
6. Kumar, M. N.; Muzzarelli, R. A.; Muzzarelli, C.; Sashiwa, H.; Domb, A. J Chem Rev 2004, 104, 6017.
7. Mi, F. L.; Tan, Y. C.; Liang, H. F.; Sung, H. W. Biomaterials 2002, 23, 181.
8. Ishihara, M.; Ono, K.; Saito, Y.; Yura, H.; Hattori, H.; Matsui, T.; Kurita, A. Int Cong Ser 2001, 1223, 251.
9. Wang, L. H.; Khor, E.; Wee, A.; Lim, L. Y. J Biomed Mater Res 2002, 63, 610.
10. Madihally, S. V.; Mattthew, H. M. T. Biomaterials 1999, 20, 1133.
11. Hench, L. L.; Wilson, J. Science 1984, 226, 630.
12. Hardy, D. C. R.; Frayssinet, P. Eur J Orthop Surg Traumatol 1999, 9, 75.
13. Shackelford, J. F. Bioceramics 1999, 293, 99.
14. Heise, U.; Osborn, J. F.; Duwe, F. Int Orthop 1990, 14, 329.
15. Best, S.; Bonfield, W. J Mater Sci Mater Med 1994, 5, 516.
16. Kong, L. J.; Gao, Y.; Cao, W. L.; Gong, Y. D.; Zhao, N. M.; Zhang, X. F. J Biomed Mater Res 2005, 75, 275.
17. Hu, Q. L.; Li, B. Q.; Wang, M.; Shen, J. C. Biomaterials 2004, 25, 779.
18. Yin, Y. J.; Zhao, F.; Song, X. F.; Yao, K. D.; Lu, W. W.; Leong, J. C. Biomaterials 2000, 77, 2929.
19. Thein-Han, W. W.; Misra, R. D. K. Acta Biomater 2009, 5, 1182.
20. Varma, H. K.; Yokogawa, Y.; Espinosa, F. F.; Kawamoto, Y.; Nishizawa, K.; Nagata, F.; Kameyama, T. Biomaterials 1999, 20, 879.
21. Yamaguchi, I.; Tokuchi, K.; Fukuzaki, H.; Koyama, Y.; Takakuda, K.; Monma, H.; Tanaka, T. J Biomed Mater Res 2001, 55, 20.
22. Zhang, L.; Li, Y. B.; Yang, A. P.; Peng, X. L.; Wang, X. J. X.; Zhang, J. Mater Sci Mater Med 2005, 16, 213.
23. Sreedhar, B.; Aparna, Y.; Sairam, M.; Neha Hebalkar, J. Appl Polym Sci 2007, 105, 928.
24. Tachaboonyakiat, W.; Serizawa, T.; Akashi, M. Polym J 2001, 33, 177.
25. Murugan, R.; Ramakrishna, S. Appl Phys Lett 2006, 88, 193124.
26. Cui, W.; Hu, Q. L.; Wu, J.; Li, B. Q.; Shen, J. C. J Appl Polym Sci 2008, 2081, 109.
27. Viala, S.; Freche, M.; Lacout, J. L. Ann Chim Sci Mater 1998, 23, 69.
28. Domard, A. Int J Biol Macromol 1987, 9, 98.
29. Lin, F. H.; Yao, C. H.; Huang, C. W.; Liu, H. C.; Sun, J. S.; Wang, C. Y. Mater Chem Phys 1996, 46, 36.
30. Brugnerotto, J.; Lizardi, J.; Goycoolea, F. M.; Arguelles-Monal, W.; Desbrieres, J.; Rinaudo, M. Polymer 2001, 42, 3569.
31. Falini, G.; Weiner, S.; Addadi, L. Calcif Tissue Int 2003, 72, 548.
32. Penel, G.; Leroy, G.; Rey, C.; Sombret, B.; Huvenne, J. P.; Bres, E. J Mater Sci Mater Med 1997, 8, 271.
33. Rehman, I.; Bonfield, W. J Mater Sci Mater Med 1997, 8, 1.
34. Wan, Y.; Creber, K. A. M.; Peppley, B.; Bui, V. T. Macromol Chem Phys 2003, 204, 850.
35. Powder Diffraction File No. 09-432, International Centre of Diffraction Data (ICDD), Newton Square, PA, USA.
36. Zhang, C. M.; Yang, J.; Quan, Z. W.; Yang, P. P.; Li, C. X.; Hou, Z. K.; Lin, J. Cryst Growth Des 2009, 9, 2725.
37. Viswanath, B.; Ravishankar, N. Biomaterials 2008, 29, 4855.
38. Sailaja, G. S.; Velayudhan, S. M.; Sunny, C.; Sreenivasan, K.; Varma, H. K.; Ramesh, P. J Mater Sci 2003, 38, 3653.
39. Wang, X. H.; Ma, J. B.; Wang, Y. N.; He, B. L. Biomaterials 2001, 22, 2247.